TECHNICAL NOTE

Is the quasi-steady state a real behaviour? A micromechanical perspective

J. YANG* and B. B. DAI*

Whether the so-called quasi-steady state is a real material response is a fundamental yet controversial question in the study of undrained shear behaviour of sand. An attempt is made here to clarify the question from a micromechanical viewpoint by means of a grain-scale modelling technique combined with statistical analyses. The study shows that the quasi-steady state is a real behaviour rather than a test-induced phenomenon; it is a transition state, and can be regarded as the result of spatial rearrangement of discrete particles sheared under the constant-volume condition. The quasi-steady state has distinct features that make it different from the steady state at both the macro scale and micro scale. During the loading process, the average number of contacts per particle decreases with strain until the quasi-steady state emerges, and after that it increases gradually to an approximately constant value at large deformations associated with the steady state. This result suggests that the loss of contacts is most pronounced at the quasi-steady state. The study also shows that the contact normal forces and particle rotations play a major role in the deformation process, whereas the contributions of contact tangential forces and particle sliding appear to be minor.

KEYWORDS: constitutive relations; fabric/structure of soils; sands

Le fait que le soi-disant état quasi-stable soit une réaction réelle du matériau est une question fondamentale, mais controversée, de l'étude du comportement du sable pour la résistance au cisaillement sans consolidation. Dans la présente communication, on s'efforce d'éclaircir ce problème sur un plan micromécanique, en employant une technique de modélisation à l'échelle du grain conjointement avec des analyses statistiques. Cette étude démontre que l'état quasi-stable est un comportement authentique plutôt qu'un phénomène induit par le test ; il s'agit d'un état transitoire, que l'on peut considérer comme un réarrangement spatial de particules discrètes cisaillées sous un volume constant. L'état quasi-stable présente des caractéristiques bien particulières qui le distinguent de l'état permanent à la macro-échelle et la micro-échelle. Au cours du processus de sollicitation, le nombre moyen de contacts par particule diminue avec la déformation sous sollicitation, jusqu'à ce qu'apparaisse l'état quasi-stable : après cela, il augmente progressivement jusqu'à une valeur à peu près constante aux grandes déformations qui se produisent dans l'état quasi-stable. Ce résultat indique que la perte de contacts est plus prononcée à l'état quasi-stable. Cette étude indique également que les forces de contact normales et les rotations de particule jouent un rôle majeur dans le processus de déformation, tandis que la contribution de forces tangentielles de contact et le glissement des particules semblent jouer un rôle mineur.

INTRODUCTION

The monotonic loading behaviour of sand under undrained conditions has been a subject of great interest in the geotechnical profession (*e.g.* Poulos, 1981; Sladen *et al.*, 1985; Vaid *et al.*, 1990; Ishihara, 1993; Been, 1999; Yang, 2002). When loose to medium dense sand is sheared under undrained conditions in triaxial tests, it frequently exhibits the response illustrated in Fig. 1, where q denotes the deviatoric stress, p is the mean effective stress and ε_1 is the axial strain. This fascinating response, sometimes referred to as limited flow failure, is characterised by a peak strength at a low strain level and a limited period of strain-softening, which is then followed by a continuous dilation to a high strength at a large mean effective stress. The transition state from increase to decrease in pore pressure is called the quasi-steady state (Alarcon-Guzman *et al.*, 1988), because it is in several aspects similar to the steady state, an ultimate state of failure in which the sand is continuously deforming at constant

volume, constant mean effective stress, constant shear stress and constant velocity (Castro, 1969; Poulos, 1981).

Many controversies exist with respect to the existence of the quasi-steady state, and cause much confusion, which hinders physical understanding. For example, questions have been raised as to the distinctions between the quasi-steady state and the steady state, and it has been argued (Been, 1999) that the erroneous linking of the quasi-steady state with the steady state (Konrad, 1990; Vaid *et al.*, 1990) caused difficulty with acceptance of the steady-state concepts in practical applications. Notably, it has been argued (Zhang & Garga, 1997) that the quasi-steady state is not a real material behaviour but a test-induced phenomenon. The major testing factors claimed to be responsible for the existence of the quasi-steady state include

(*a*) end restraint or end friction
(*b*) non-uniform deformation
(*c*) membrane penetration
(*d*) sample dimensions correction.

Obviously these factors are interrelated, and among them the end restraint is considered the most fundamental.

In a conventional triaxial setting the friction between the sample and the end platens during shearing may influence the dilation potential of the sample in the end zones, and
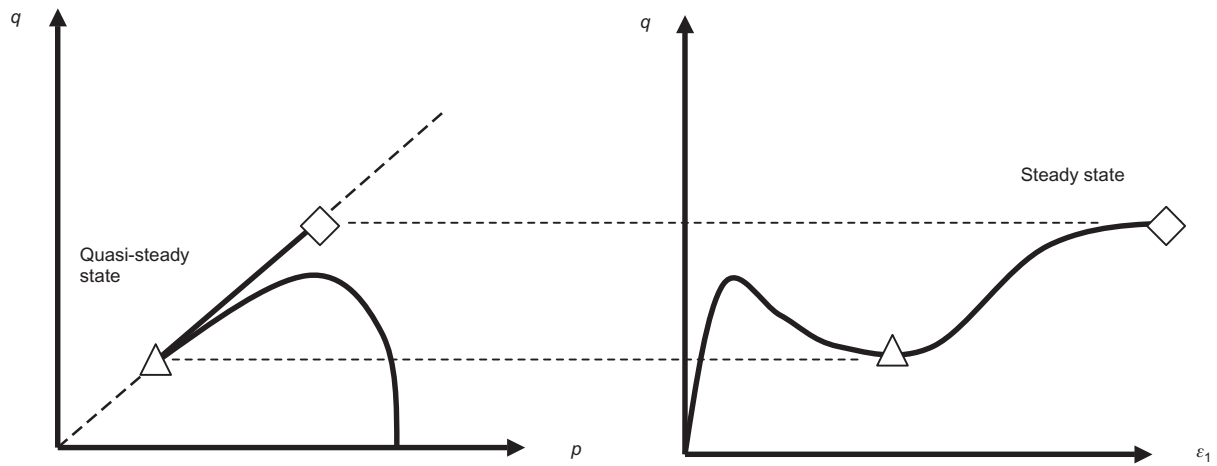
Fig. 1. Undrained shear behaviour of sand exhibiting quasi-steady state

cause bulging deformations in the sample. As a consequence, the pore pressure in the sample may tend to decrease and the deviatoric stress may tend to increase, accompanied by a continuous dilation and strain-hardening response. Much debate, however, surrounds this argument, because it is thought that the effect of end restraint is negligible if lubricated end platens are used properly (Vaid *et al.*, 1999; Yoshimine, 1999). Using their triaxial test data Vaid *et al.* (1999) have shown that the quasi-steady state existed regardless of whether the end platens were frictionless or frictional (Fig. 2).

While accepting that the lubricated platens are effective in reducing the end restraint effect, one may still be confused by the observation in Fig. 2, which shows that the end friction indeed exerts influence on the mechanical behaviour of sand samples, and that the quasi-steady state appears to be more obvious for frictional end platens. Physically, it is difficult, if not impossible, to eliminate all unfavourable impacts on experimental results that may be induced by testing procedures. It thus becomes highly desirable to explore the quasi-steady state in a way that is different from the conventional laboratory experiments, and is free from the friction effect. This is precisely the motivation of the present study.

From the mechanical point of view, the fascinating point in relation to the quasi-steady state is as follows: How can a sand sample, after 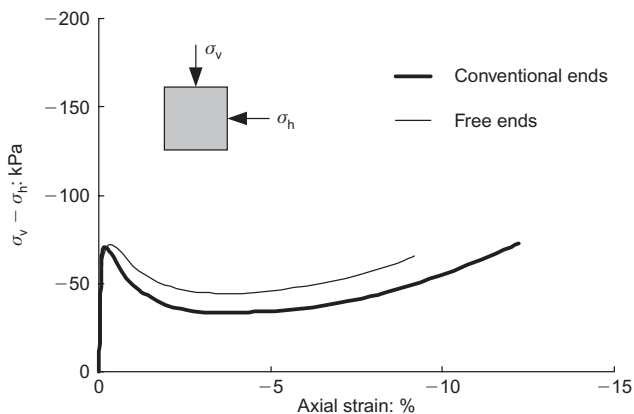collapse, regain a strength that is even higher than its peak strength at significantly large deformations? Here, the phenomenon is considered to originate from the discrete nature of sand. That is to say, the macroscale behaviour observed in the laboratory and in situ is dependent not only on the interaction among the discrete particles but also on how these particles are packed in the space, and on how the packing pattern evolves during the loading process. In this context, an attempt is made here, by means of a grain-scale modelling technique, to explore whether the quasi-steady state is a fundamental material behaviour. This technique, known as the discrete or distinct element method (Cundall & Strack, 1979), is based on the concept that the particles of a granular soil assembly displace only through interactions with each other at contact points. It has emerged in recent years as a promising tool in the study of the mechanical behaviour of granular soils (e.g. Thornton, 2000; Bolton *et al.*, 2008, and the references therein).

MODELLING OF GRANULAR SOIL ASSEMBLIES

The general principle of the discrete element method is that the quasi-static deformation behaviour of an assembly of particles is studied by monitoring the interactions of particles contact by contact, and the system of equations describing the dynamic interactions of particles is solved using an explicit time-stepping scheme. Several computer codes adopting the principle have been developed; in this study the two-dimensional program PFC2D (Itasca, 2005) is used because of its widely recognised computational performance. Detailed discussion of the method and the program is beyond the scope of this paper. Only key information relating to the modelling is briefly described below.

First, this study adopts a simple contact constitutive model, assuming a linear relation between the contact forces and the displacements, and applying the Coulomb friction criterion at the contact. A no-tension condition is assumed at the contact, which is considered adequate for clean sand without interparticle cementation or bonding.

Second, to allow for realistic particle shapes, clumped particles, each consisting of two partly overlapped disc-shaped particles (see the insert in Fig. 3(a)), are produced. The aspect ratio of each clump, defined as the ratio between the diameter of the constituent disc and the distance of the long axis of the clumped particle, is assigned a value of 0·6. An equivalent particle diameter is then introduced as the diameter of a circular particle having the same area as the clump, and the range of the equivalent diameter is specified
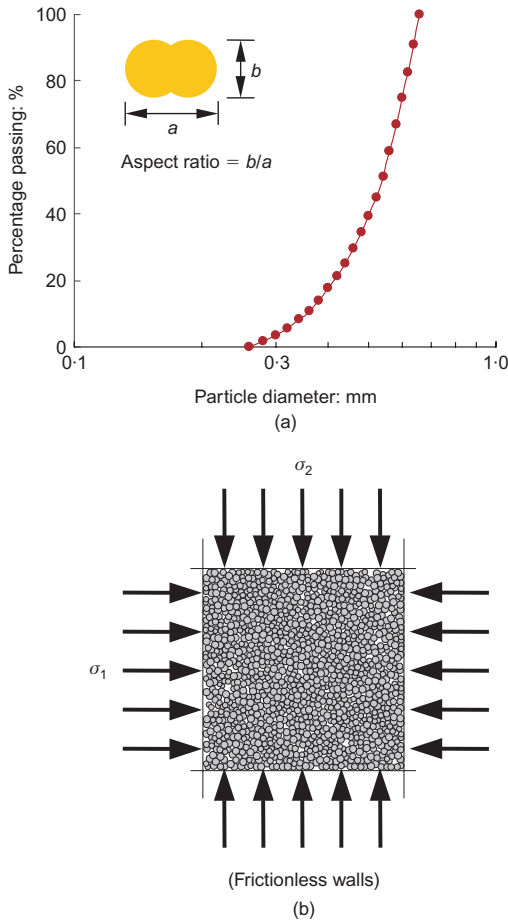

Fig. 2. Undrained response of loose Fraser River sand in triaxial extension with conventional and free ends (after Vaid *et al.*, 1999)

Fig. 3. Particle shape and particle size distribution used in biaxial shear

to vary between 0·26 and 0·66 mm. The particle grading curve formed in this way is given in Fig. 3(a), indicating that the granular assembly can be categorised as medium to fine sand.

Each clumped particle is assumed to behave as a rigid body, with a deformable boundary only, and to not break apart. In this connection, a clump differs from a group of particles that are bonded to one another and thus have the possibility of breaking apart. All the particles are attributed with the following properties: normal and tangential stiffness $= 10^9$ N/m; mass density $= 2650$ kg/m^3; and coefficient of interparticle friction $= 0·5$.

The numerical sample, formed by the gravitational deposition, has dimensions of 25 mm $\times$ 25 mm and contains about 2800 particles (Fig. 3(b)). The sample is isotropically compressed to 1000 kPa at a void ratio of 0·217, and then is subjected to a deviatoric shear. The undrained condition is simulated by performing the test under the constant-volume condition. Note that the friction between the four boundary walls and particles is assumed to be zero, to eliminate all boundary friction effects.

RESULTS OF SIMULATIONS
Deformation behaviour at the macroscale

Figure 4(a) shows the evolution of the deviatoric stress, $q = (\sigma_1 - \sigma_2)$, with the axial strain in the horizontal direction. The evolution of the deviatoric stress with the mean normal stress, $p = (\sigma_1 + \sigma_2)/2$, is shown in Fig. 4(b). Qualitatively these figures show a response that is typical of that obtained in the laboratory for loose to medium dense sand samples under undrained shear conditions. In particular,

they clearly show the existence of the quasi-steady state: initially the deviatoric stress increases with strain, and arrives at a peak strength of about 450 kPa; the strain-softening response then follows, but ceases at about 2·5% strain, with a minimum strength of 380 kPa; after that the sample exhibits a continuous strain-hardening behaviour to reach a strength of as high as 4300 kPa at the 30% strain level. Correspondingly, the mean normal stress also takes a minimum and then climbs up to 4900 kPa at large strains (Fig. 4(c)).

The evolution of the stress ratio q/p with deformations is shown in Fig. 4(d). It is observed that the stress ratio increases almost linearly until the strain level at which the peak deviatoric stress occurs; after that the rate of change of the stress ratio drops to a significantly lower value. The stress ratio q/p reaches an essentially constant value at large deformations. It is worth noting that, given the constant-volume condition, this constant stress ratio ($\sim 0·88$) approximately satisfies the Rowe's stress–dilatancy relationship (Rowe, 1962)

$$\frac{\sigma_1}{\sigma_2} \frac{1}{1 + d\dot{V}/V\dot{\varepsilon}_1} = \tan^2\left(45 + \frac{\phi_\mu}{2}\right) \tag{1}$$

where ϕ_μ is taken as the angle of interparticle friction ($\sim 26·6°$). However, this observation may not remain valid if the particle properties (e.g. particle shape and interparticle friction) vary. Further work to clarify this issue will be reported in a future paper.

Microscale characteristics of particle and contact orientations

The particle orientation and contact orientation are two useful quantities characterising the spatial arrangement of particles in an assembly (i.e. fabric). It is thus of interest to examine how they evolve with deformations. For the two-dimensional case considered, an angular distribution function (Oda, 1982; Rothenberg & Bathurst, 1989) can be introduced to describe the characteristics of a fabric

$$E(\phi) = E_0[1 + a_n \cos 2(\phi - \phi_n)] \tag{2}$$

with $0 \leqslant \phi \leqslant 2\pi$. Here E_0 denotes the distribution density at the isotropic state, a_n is a parameter defining the magnitude of anisotropy and ϕ_n defines the principal direction of the fabric.

The computed principal directions of particle and contact orientations are shown as a function of strain in Fig. 5. The principal direction of particle orientations (i.e. the major axis of elongation) is at about 80° to the vertical direction at the initial state, and it decreases continuously until an essentially constant value close to 0° is reached at large strains. This means that particles orient along the minor principal stress direction at large strains. The principal direction of contact normal orientations, on the other hand, is approximately along the vertical direction before shearing, but it changes drastically to the horizontal direction at a very small strain, and then remains almost unchanged during the subsequent shearing.

It seems that the quasi-steady state does not show distinct features in the evolutions of particle and contact orientations. However, by examining the number of contacts per particle in the assembly (i.e. the coordination number), it is found that the number approximately takes a minimum ($\sim 3·92$) at the quasi-steady state, as shown in Fig. 5(c). Before the quasi-steady state emerges, the coordination number decreases with strain, and after that it increases with strain until an approximately constant value ($\sim 4·66$) is reached at large deformations.
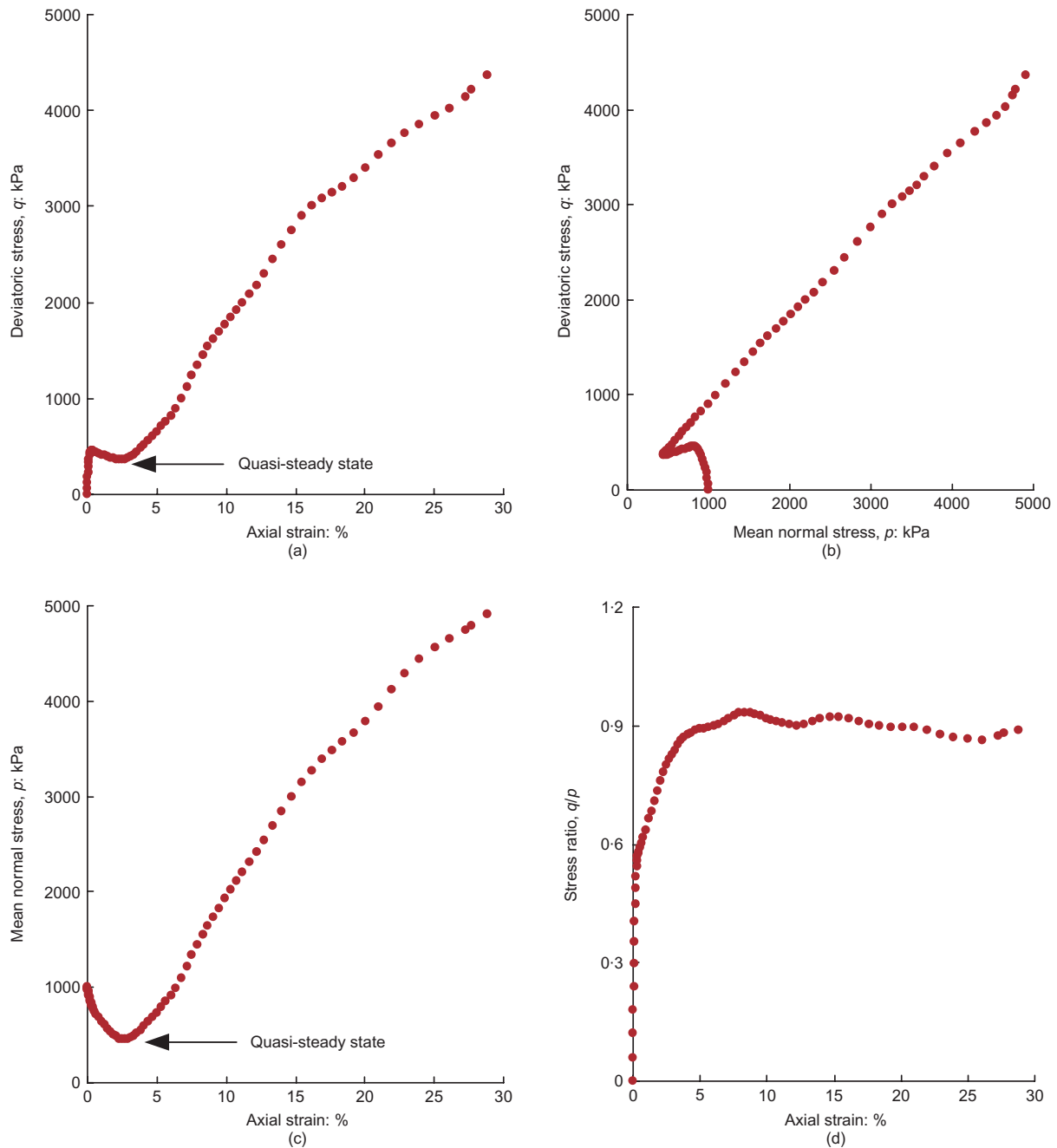
Fig. 4. Macroscale shear behaviour under constant-volume condition

Interesting comparisons of the rose diagrams of particle and contact orientations at the initial state, quasi-steady state and steady state are given in Fig. 6. The spatial distribution of particle orientations at the quasi-steady state, as compared with that at the initial state, is essentially identical, whereas the principal direction of the contact orientations changes by 90°. This change actually occurs well before the quasi-steady state emerges. Furthermore, particle orientations at the steady state exhibit a markedly different feature from those at the initial state and quasi-steady state, with the principal direction of particle orientations being rotated through 90°. This means that the principal direction changes from the horizontal at the initial state to the vertical at the steady state. Both the spatial distribution of particle orientations and that of contact orientations become peanut-shaped at the steady state (Fig. 6(c)).

Microscale characteristics of contact forces

The magnitudes of contact forces in the assembly may vary from contact to contact. Nevertheless, when the normal and tangential components of contact forces are averaged over the assembly, their variations may show characteristic trends. To explore these trends at different stages of deformations, two angular distribution functions, similar to that in equation (2), are introduced to characterise the anisotropy of contact normal force and contact tangential force.

Figure 7 shows the distributions of average normal forces and tangential forces at the initial state, quasi-steady state and steady state. The spatial distribution of average normal forces is essentially isotropic at the initial state. By comparison, the average tangential forces are much smaller in magnitude, and their spatial distribution shows clear orientations along lines of 45° and 135°.
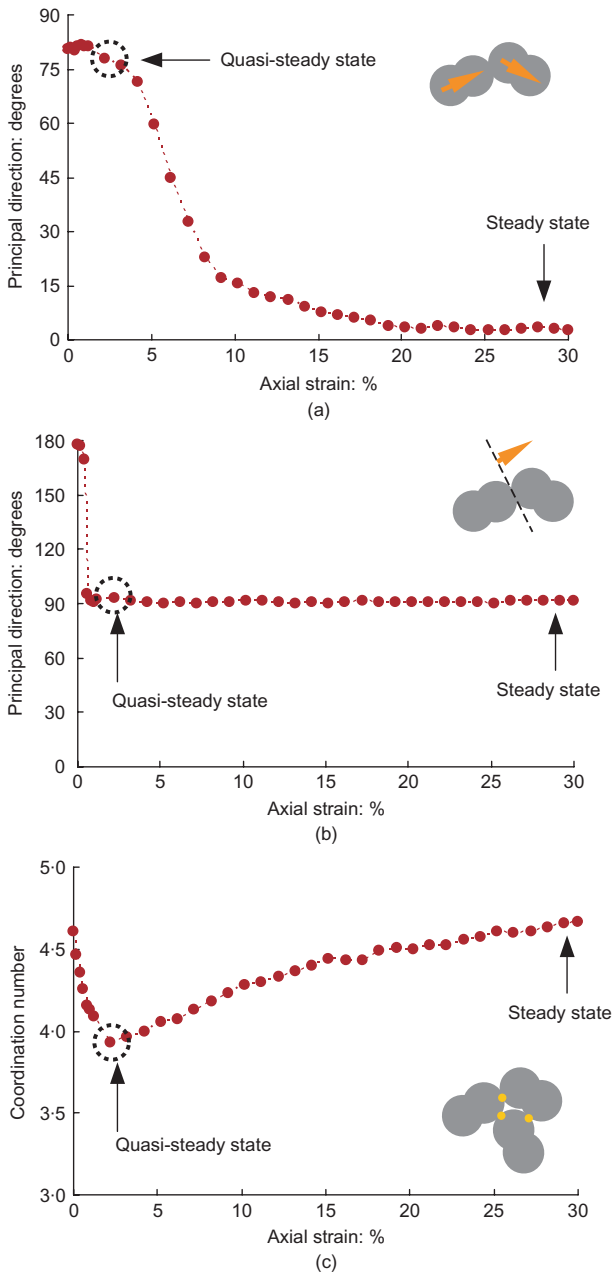
Fig. 5. Evolutions of micro properties during shear: (a) particle orientation; (b) contact normal orientation; (c) coordination number

At the quasi-steady state, the distribution of average normal forces exhibits a strong anisotropy (Fig. 7(b)): the maximum average normal forces are carried by contacts with orientations close to the direction of major principal stress. The magnitudes of average normal forces decrease signifi-

cantly when the sample is sheared to the quasi-steady state. By comparison, the maximum average tangential forces are almost doubled in magnitude from those at the initial state, with the angular distribution unchanged.

At the steady state, the principal direction of average normal forces remains the same as that at the quasi-steady state. But it should be noted that the maximum average normal and tangential forces at the steady state are about 10 times those at the quasi-steady state.

Figure 8 shows the displacement vectors at the quasi-steady state and steady state. The sample remains essentially square-shaped at the quasi-steady state, but is changed to be rectangular at the steady state. No strong shear-banding feature or bulging deformation pattern emerges at either state. Statistics show that the percentage of sliding contacts, defined as the ratio between the number of contacts where sliding occurs and the number of total contacts, is about 3·45% at the quasi-steady state and about 2·87% at the steady state. This suggests that friction sliding may not be a major contributor to the evolution of the packing structure. On the other hand, it is found that at the quasi-steady state less than 7% of particles rotate over 10° (with reference to the initial state), whereas at the steady state more than 70% of particles rotate over 10°. The details of the statistics for the two characteristic states are given in Table 1.

FURTHER DISCUSSION
The quasi-steady state generally pertains to loose to medium dense sand subjected to undrained shear. If the same sand becomes even looser it may exhibit a flow-type response: this response has been observed in many laboratory tests (e.g. Yang, 2002, and the references therein). It is thus of interest to examine whether this flow-type response will occur if the void ratio of the assembly of particles becomes larger but loaded under otherwise identical conditions. In so doing, a sample having a void ratio of 0·239 is prepared and then subjected to the same deviatoric loading conditions. The simulation results are shown in Fig. 9(a) in terms of the q–p relationship. For purposes of comparison, the earlier results for the sample $e = 0·217$ are superimposed on the figure.

When the sample becomes looser, it clearly shows a flow-type response: the deviatoric stress quickly drops from a peak value at a small strain to zero, accompanied by a decrease of mean normal stress. More interestingly, a straight line passing through the origin can be sketched out along which both samples are sheared to failure. This result is in good agreement with the observations from many real laboratory tests (e.g. Ishihara, 1993). In the framework of critical state soil mechanics, the straight line can be regarded as the critical state line in the stress space. To further verify this point, an additional sample having a void ratio of 0·217 but subjected to an isotropic stress of 500 kPa is prepared for subsequent shearing under otherwise identical conditions. Fig. 9(b) compares its stress path with that for $e = 0·217$

Table 1. Statistics of microstructural parameters at characteristic states

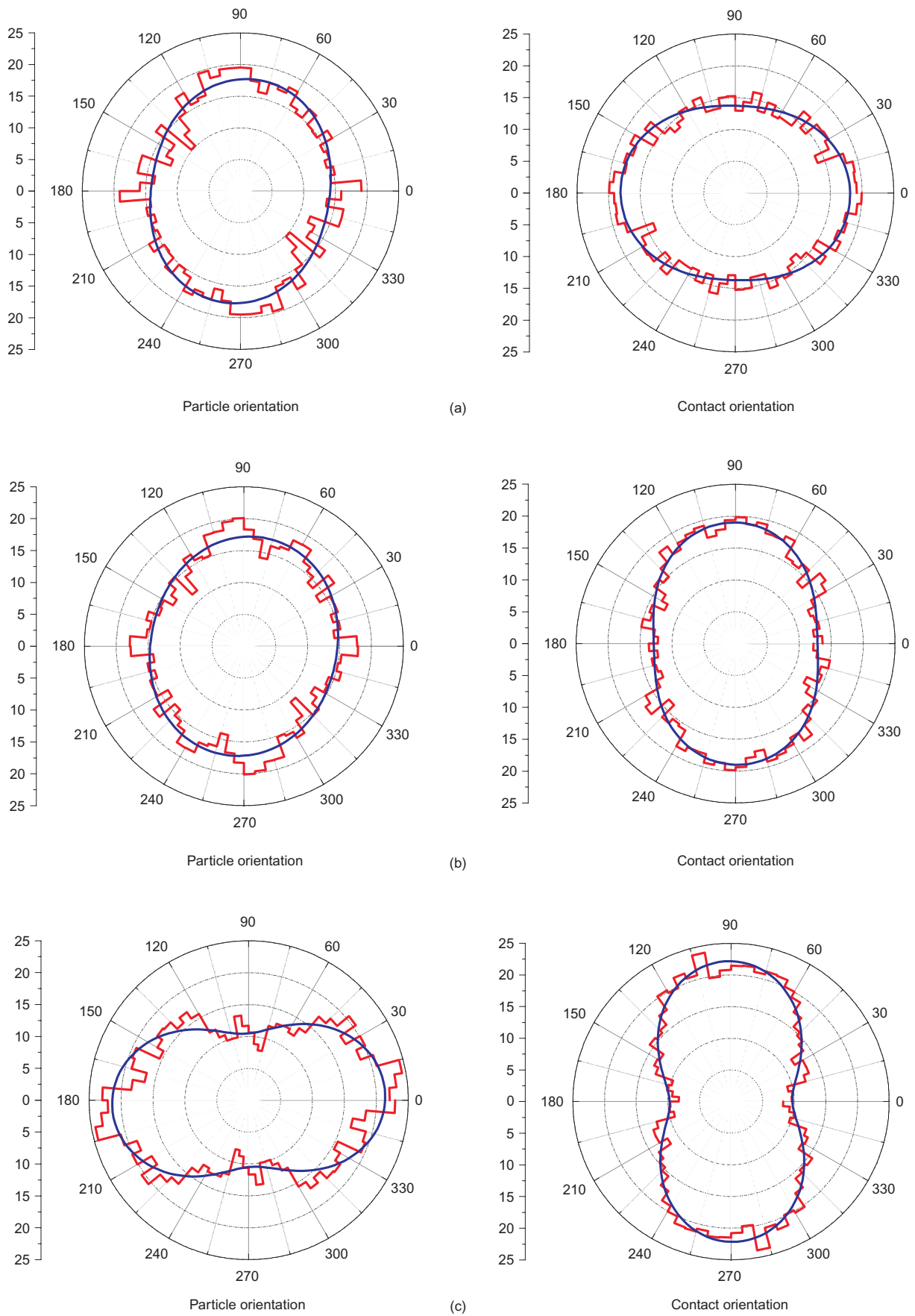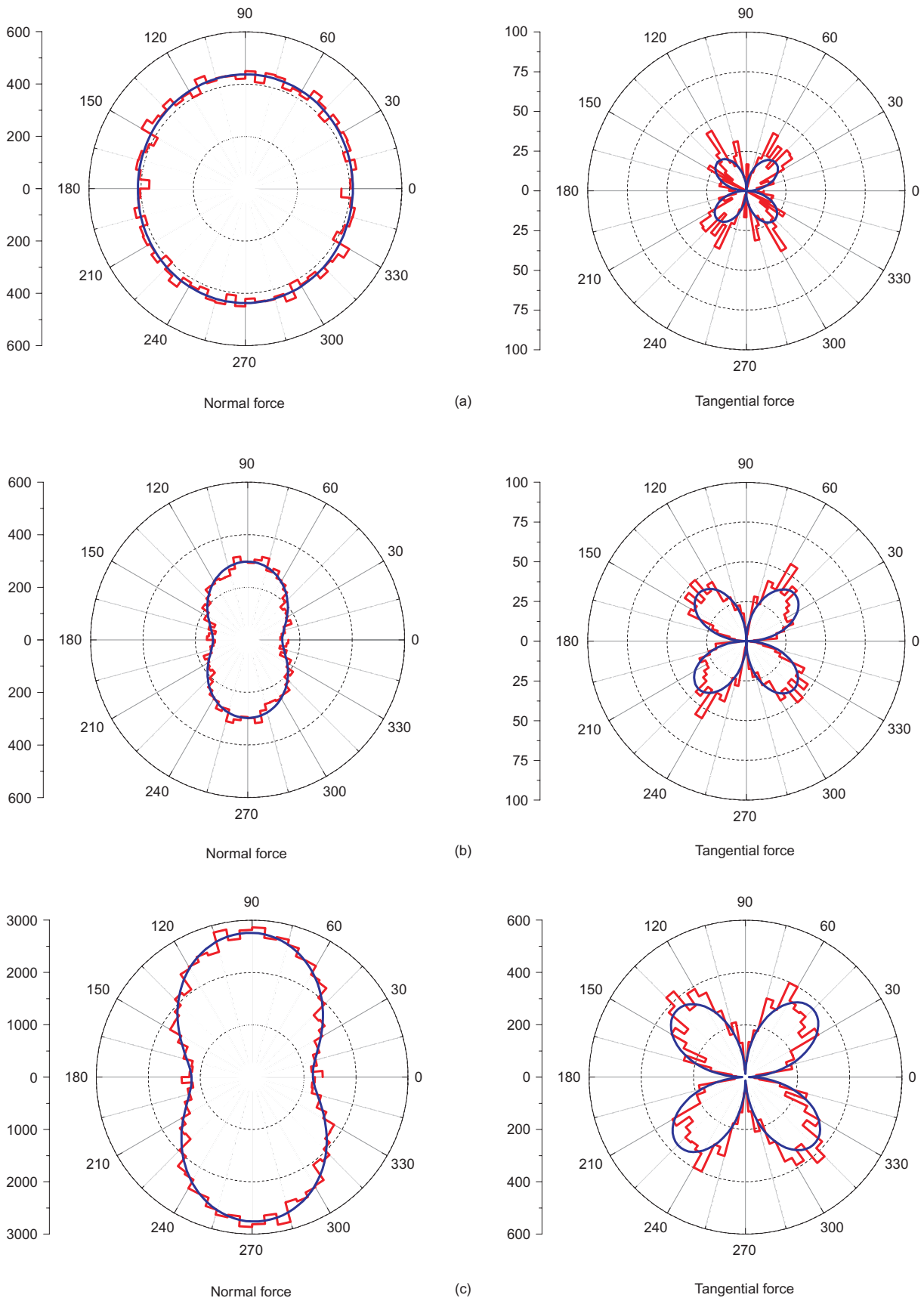|	Coordination number	Percentage of sliding contacts: %	Distribution of particle rotations: %		
			$< 5°$	$> 5°$ and $< 10°$	$> 10°$
Initial state	4·61	—	—	—	—
Quasi-steady state	3·94	3·82	81·1	12·1	6·8
Steady state	4·60	2·87	13·6	12·7	73·7

Fig. 6. Distributions of particle and contact orientations at different stages: (a) initial state; (b) quasi-steady state; (c) steady state (density in per cent)

Fig. 7. Distributions of contact normal force and tangential force at different stages: (a) initial state; (b) quasi-steady state; (c) steady state (units of forces: N)
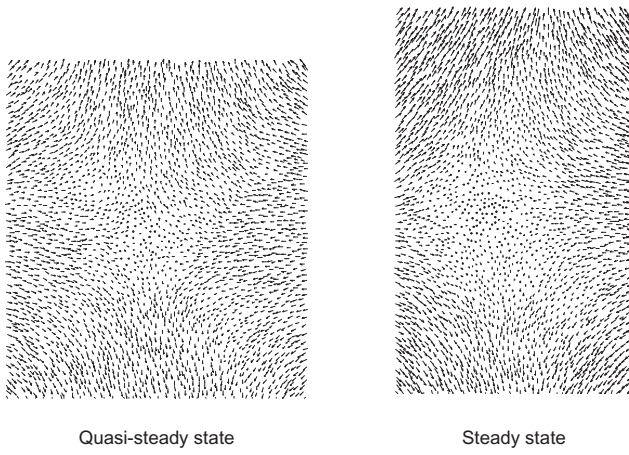
Quasi-steady state   Steady state

Fig. 8. Displacement fields at quasi-steady state and steady state

and $p = 1000$ kPa. It is encouraging to see that the same critical state line can be drawn.

The evolution of the contact number in the flow-type response is compared with that in the quasi-steady state type response in Fig. 9(c). In the former case the number of contacts drops drastically when the shear starts, without any regain of the number of contacts as in the quasi-steady state type response. This represents a very significant loss of contacts in the flow-type response. Moreover, it is observed that the deformation of the looser sample is limited: this is because the equilibrium criterion based on unbalanced forces cannot be satisfied at larger deformations in the simulation. In these respects, the assembly reaches an unstable state similar to that of sand in liquefaction.

As far as the case of $e = 0.217$ and $p = 500$ kPa is concerned, the evolutions of contact numbers approximately share the same pattern with that of the case $e = 0.217$ and $p = 1000$ kPa, with the coordination number reaching a
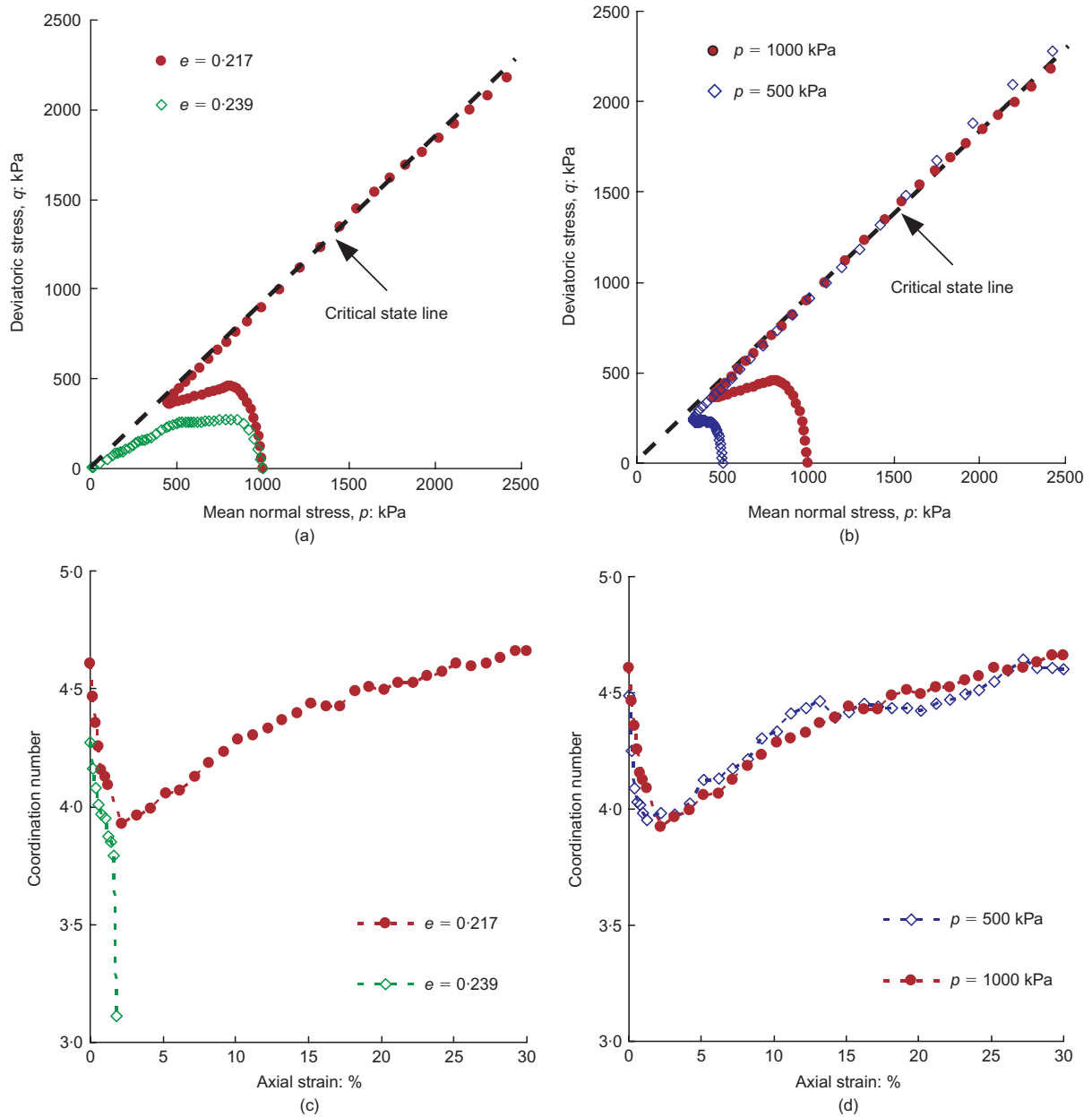

Fig. 9. Effects of void ratio and confining stress on: (a) and (b) macroscale response; (c) and (d) evolutions of coordination number

minimum at the quasi-steady state where the mean normal stress also takes a minimum (Figs 9(b) and 9(d)). The implication is that the coordination number is closely related to the effective mean normal stress during the loading process.

Although the particle shape and contact laws in the modelling differ to some extent from real soil particles, the results of simulations show reasonable agreement with the observations from real laboratory tests in several key aspects, and provide a useful microscopic insight into the complex behaviour of granular soils. Further work taking into consideration different particle shapes, contact laws and three-dimensional effects would be of value in enhancing the understanding derived.

SUMMARY AND CONCLUSIONS

An attempt has been made to probe into the nature of the quasi-steady state in undrained shear of granular soils. The main results of the study can be summarised as follows.

(a) The quasi-steady state is a real material behaviour rather than a test-induced phenomenon. At the grain scale it can be regarded as the result of spatial rearrangement of discrete particles under the constant-volume shearing condition. At the macroscale it is a transition state from the post-peak strain-softening to a continuous strain-hardening response.

(b) In the evolutions of particle and contact orientations, the quasi-steady state does not show characteristic features. The coordination number at the quasi-steady state, however, marks a clear boundary in the process: it decreases with strain before the state emerges, and then increases with strain until an approximately constant value is reached at large deformations. This result suggests that the loss of contacts is most pronounced at the quasi-steady state.

(c) At the quasi-steady state the maximum normal forces, on average, are carried by contacts with orientations close to the direction of the major principal stress. The maximum average normal forces are smaller than those at the initial state, whereas the maximum average tangential forces are larger than those at the initial state.

(d) The quasi-steady state also differs from the steady state in respect of the contact forces. Both the normal and tangential components at the steady state are significantly larger than those at the quasi-steady state. Particles are oriented approximately along the direction of the minor principal stress at the steady state, but only at a small deviation from the direction of the major principal stress at the quasi-steady state.

(e) During shear deformations the average tangential forces at contacts are always much smaller than the average normal forces, and the number of contacts where sliding occurs is always small. This result suggests that the tangential forces are not a major contributor to spatial rearrangement of particles; rather, the contact normal forces and particle rotations play a major role.

ACKNOWLEDGEMENTS

NOTATION

a distance of the long axis of the clumped particle
a_n parameter defining the magnitude of anisotropy
b diameter of the constituent disc
E_0 distribution density at the isotropic state
e void ratio
p mean effective stress
q deviatoric stress
$d\dot{V}/V$ rate of unit volume change (Eq. (1))
ε_1 axial strain
$\dot{\varepsilon}_1$ rate of major principal strain change (Eq. (1))
σ_h horizontal stress (Fig. 2)
σ_v vertical stress (Fig. 2)
σ_1 major principal stress
σ_2 minor principal stress
ϕ_n principal direction of the fabric
ϕ_μ angle of interparticle friction

REFERENCES

Alarcon-Guzman, A., Leonards, G. & Chamean, J. L. (1988). Undrained monotonic and cyclic strength of sands. *J. Geotech. Engng ASCE* **114**, No. 10, 1089–1109.

Been, K. (1999). The critical state line and its application to soil liquefaction. In *Physics and mechanics of soil liquefaction* (eds P. V. Lade and J. A. Yamamuro), pp. 195–204. Rotterdam: Balkema.

Bolton, M. D., Nakata, Y. & Cheng, Y. P. (2008). Micro- and macro-mechanical behaviour of DEM crushable materials. *Géotechnique* **58**, No. 6, 471–480, **doi**: 10.1680/geot.2008.58.6.471.

Castro, G. (1969). *Liquefaction of sands*. PhD thesis, Harvard University, Cambridge, MA.

Cundall, P. A. & Strack, O. D. L. (1979). A discrete numerical model for granular assemblies. *Géotechnique* **29**, No. 1, 47–65, **doi**: 10.1680/geot.1979.29.1.47.

Ishihara, K. (1993). Liquefaction and flow failure during earthquakes. *Géotechnique* **43**, No. 3, 351–415, **doi**: 10.1680/geot.1993.43.3.351.

Itasca (2005). *User's manual for PFC2D*. Minneapolis, MN: Itasca Consulting Group, Inc.

Konrad, J. M. (1990). Minimum undrained strength versus steady-state strength of sands. *J. Geotech. Engng ASCE* **116**, No. 6, 948–963.

Oda, M. (1982). Fabric tensor for discontinuous geological materials. *Soils Found.* **22**, No. 4, 96–108.

Poulos, S. J. (1981). The steady state of deformation. *J. Geotech. Engng Div. ASCE* **107**, No. 5, 553–562.

Rothenberg, L. & Bathurst, R. J. (1989). Analytical study of induced anisotropy in idealized granular materials. *Géotechnique* **39**, No. 4, 601–614, **doi**: 10.1680/geot.1989.39.4.601.

Rowe, P. W. (1962). The stress–dilatancy relation for static equilibrium of an assembly of particles in contact. *Proc. R. Soc. London A* **269**, 500–527.

Sladen, J. A., D'Hollander, R. D. & Krahn, J. (1985). The liquefaction of sands, a collapse surface approach. *Can. Geotech. J.* **22**, No. 4, 564–578.

Thornton, C. (2000). Numerical simulations of deviatoric shear deformation of granular media. *Géotechnique* **50**, No. 1, 43–53, **doi**: 10.1680/geot.2000.50.1.43.

Vaid, Y. P., Chung, E. K. F. & Kuerbis, R. H. (1990). Stress path and steady state. *Can. Geotech. J.* **27**, No. 1, 1–7.

Vaid, Y. P., Eliadorani, A., Sivathayalan, S. & Uthayakumar, M. (1999). Quasi-steady state: a real behavior? Discussion. *Can. Geotech. J.* **36**, No. 1, 182–183.

Yang, J. (2002). Non-uniqueness of liquefaction line for loose sand. *Géotechnique* **52**, No. 10, 757–760, **doi**: 10.1680/geot.2002.52.10.757.

Yoshimine, M. (1999). Quasi-steady state: a real behavior? Discussion. *Can. Geotech. J.* **36**, No. 1, 186–187.

Zhang, H. & Garga, V. K. (1997). Quasi-steady state: a real behavior? *Can. Geotech. J.* **34**, No. 5, 749–761.